

**TRACTIVE FORCE FLUCTUATIONS
AROUND AN OPEN CHANNEL
PERIMETER AS DETERMINED FROM
POINT VELOCITY MEASUREMENTS**

by

Phillip "F." Enger

**A paper to be presented at the
ASCE Convention Phoenix,
Arizona, April 10-14, 1961**

TRACTIVE FORCE FLUCTUATIONS AROUND AN
OPEN CHANNEL PERIMETER AS DETERMINED
FROM POINT VELOCITY MEASUREMENTS

by

Phillip "F." Enger*

SYNOPSIS

The study described was conducted primarily to investigate the possibility of using point velocities occurring in an open channel to determine the tractive force (boundary shear) distribution on the perimeter of the channel.

In a straight trapezoidal channel constructed with a well-graded sand-gravel boundary, various discharges were established and vertical velocity traverses were obtained. Velocities were obtained by use of Pitot banks, and were plotted and shown to follow a logarithmic formula. Using von Karman's logarithmic velocity distribution law, the boundary shear distribution was calculated from the velocity distribution. The average of this boundary shear was determined and compared with the average obtained from du Boys formula. General agreement of the two averages is indicated at all discharges.

The mathematical method of least squares was used to fit a quadratic tractive force distribution curve to the data. The data indicate boundary shears distributed around the perimeter of the channel tested

*Hydraulic Engineer, Hydraulic Laboratory, Bureau of Reclamation, Denver Federal Center, Denver, Colorado.

fluctuated considerably. A deviation of the tractive force fluctuations from the average curve was calculated.

INTRODUCTION

Although the practice of excavating channels in earth and conducting water through them goes beyond the beginning of recorded history, there are some phases of this science which are not fully understood. One of these includes the distribution of forces acting on the channel boundary due to the flowing water, and stability of the boundary as a result of these forces.

Fluid forces acting on a channel boundary are termed tractive forces. Knowledge of their distribution and magnitude around a channel perimeter is important if a stable design through a given material is desired.

In the past, many investigators have been concerned with developing equations for velocity distributions in turbulent flow. This study was made to investigate the possibility of using the resultant formula to determine the tractive force distribution on the perimeter of an open channel.

For this study, a trapezoidal-shaped channel of a well graded sand-gravel mixture was formed, and point velocity traverses were obtained

for several discharges. Computations of boundary shear conditions were made from these point velocities.

SHORT BACKGROUND AND APPROACH TO THE PROBLEM

In the late 19th Century, Osborne Reynolds expressed the apparent shearing stress between parallel planes in the flow due to transfer of momentum as:

$$\tau_{xy} = -\rho \overline{u'v'}$$

where

τ_{xy} = shearing stress between planes

ρ = density of the fluid (neglecting variations)

u' = velocity fluctuation in direction of flow

v' = velocity fluctuation perpendicular to direction of flow

The bar indicates mean values, and the negative sign is used because of the general association of positive v' with negative u' and negative v' with positive u' .

These turbulent stresses are so large in comparison to laminar friction that laminar friction is usually neglected in turbulent flow, except in the "laminar sublayer" where laminar friction is predominant.

Prandtl (1)* introduced the idea of a "mean free path" or "mixing length," ℓ , defined as the average distance, perpendicular to the

*Numbers refer to bibliography.

main flow, traveled by a particle before it accommodates itself to new surroundings. Prandtl assumed u' proportional to $l \frac{du}{dy}$, the mixing length and the velocity gradient, and $|v'|$ proportional to $|u'|$. He then wrote the equation for the shear stress, by simple substitution as:

$$\tau_{xy} = \rho l^2 \left(\frac{du}{dy} \right)^2$$

In the preceding assumption and following assumptions, l is necessarily assumed to be small.

To determine the mixing length, von Karman (2) assumed that the turbulent exchange was independent of the viscosity and the local flow pattern was statistically similar at every point with only time and length scales varying. Using these assumptions, he set the mixing length proportional to:

$$\left| \frac{\frac{du}{dy}}{\frac{d^2u}{dy^2}} \right|$$

or

$$l = \kappa \left| \frac{\frac{du}{dy}}{\frac{d^2u}{dy^2}} \right|$$

Substituting into the shear stress formula results in:

$$\tau_{xy} = \kappa^2 \rho \frac{\left(\frac{du}{dy} \right)^3}{\left(\frac{d^2u}{dy^2} \right)^2}$$

or

$$\frac{\kappa}{\sqrt{\frac{\tau_{xy}}{\rho}}} = \frac{\left(\frac{d^2u}{dy^2} \right)}{\left(\frac{du}{dy} \right)^2}$$

Replacing τ_{xy} by its value at the boundary, τ_0 , and finding one solution for the differential equation results in:

$$u = \frac{1}{\kappa} \sqrt{\frac{\tau_0}{\rho}} \ln \frac{y + \epsilon}{\delta}$$

where

ϵ = a constant having dimension of a length, is small in comparison with y and is neglected.

δ = a constant having dimensions of a length.

The preceding equation written in the form of:

$$u = \frac{1}{\kappa} \sqrt{\frac{\tau_0}{\rho}} \ln \frac{y}{\delta}$$

is considered the "universal velocity distribution near the wall," and is developed as a function of the distance from the wall as:

$$u = \frac{1}{\kappa} \sqrt{\frac{\tau_0}{\rho}} \ln y + f(y)$$

where $f(y)$ depends on the fluid viscosity or the roughness of the wall.

Von Karmen determined the best value of κ to be 0.4, and Keulegan (3) developed the equation for open channels with smooth walls as:

$$\frac{u}{u_*} = 5.5 + 5.75 \log \left(\frac{y + u_*}{\nu} \right)$$

and for rough walls as:

$$\frac{u}{u_*} = 8.5 + 5.75 \log \left(\frac{y}{k_s} \right)$$

where:

$$u_* = \sqrt{\frac{\tau_0}{\rho}}$$

k_s = a roughness factor.

Einstein (4) combined Keulegan's formulas into one general formula covering smooth and rough walls by writing them in the form:

$$\frac{u_y}{u_*} = 5.75 \log \left(\frac{30.2 y \chi}{k_s} \right) = 5.75 \log \left(\frac{30.2 y}{\Delta} \right)$$

where:

$$\chi = f\left(\frac{k_s}{\delta}\right) \text{ a corrective parameter}$$

$$\Delta = \frac{k_s}{\chi}$$

Using this general equation in the form:

$$\frac{u_y}{u_*} = C \log \left(\frac{C_1 y}{\Delta} \right)$$

and writing the equation for two points near the bed and in the range

where the equation expresses the velocity distribution results in:

$$\frac{u_{y_2}}{u_*} = C \log \left(\frac{C_1 y_2}{\Delta_2} \right)$$

$$\frac{u_{y_1}}{u_*} = C \log \left(\frac{C_1 y_1}{\Delta_1} \right)$$

where:

$$y_2 > y_1$$

$$\Delta_2 = \Delta_1$$

Subtracting the velocity at y_1 from that at y_2

$$u_{y_2} - u_{y_1} = u_* C \left[\log \frac{C_1 y_2}{\Delta} - \log \frac{C_1 y_1}{\Delta} \right]$$

and writing the last term as

$$\log C_1 + \log y_2 - \log \Delta - \log C_1 - \log y_1 + \log \Delta$$

and canceling, results in

$$\log y_2 - \log y_1 = \log \left(\frac{y_2}{y_1} \right)$$

The equation now assumes the form:

$$u_{y_2} - u_{y_1} = u_* C \log \left(\frac{y_2}{y_1} \right)$$

Solving for τ_o

$$\tau_o = \rho \left[\frac{u_{y_2} - u_{y_1}}{C \log \frac{y_2}{y_1}} \right]^2$$

This equation can be simplified if y_2 and y_1 are used as constants giving:

$$\tau_o = C_2 (u_{y_2} - u_{y_1})^2$$

where:

$$C_2 = \frac{\rho}{\left[5.75 \log \frac{y_2}{y_1} \right]^2}$$

If y_2 and y_1 are chosen to result in $C_2 = 1$ the equation is further simplified.

This equation indicates that boundary shear at the bed, commonly called tractive force, varies with the square of the velocity gradient, and that by choosing two points from the velocity gradient the shear at the boundary can be determined.

The equation is, of course, limited to the assumptions made in the basic derivations.

This equation was used to establish the tractive force distribution around the perimeter of the trapezoidal channel. To check the results,

the average tractive force was also obtained from the du Boys formula, which can be derived as follows:

If water is flowing through a channel with a constant cross section, A, the total weight of the water volume over a length L is:

$$W = A \gamma L$$

where: γ = unit weight of water

The force acting normal to the channel slope is $W_n = A \gamma L \cos \alpha$

where: $\tan \alpha$ is the slope of the channel bottom. The total force acting along the slope is:

$$F = \gamma A L \sin \alpha$$

This force may be expressed as a force per unit area by dividing by the wetted perimeter, P, and the length over which it acts, L. This will be recognized as the average boundary shear, or tractive force τ_a .

$$\tau_a = \frac{\gamma A}{P} \sin \alpha$$

Noting $\frac{A}{P}$ is equal to the hydraulic radius, and that for small angles $\sin \alpha$ is approximately equal to $\tan \alpha$, or the canal slope, the formula results in:

$$\tau_a = \gamma R S$$

For wide rivers R is approximately equal to the depth, d, and for nonuniform flow the slope of the energy gradient is used in the formula.

TEST EQUIPMENT

A laboratory test flume 72 feet long, 8 feet wide, and 24 inches deep, Figures 1, 2, and 3, was used for the study. Two to one side slopes made of wooden framework covered with a concrete mix were built into the flume. Over the side slopes and on the channel bottom, a sand-gravel mixture, analysis curve shown in Figure 4, was placed. The channel section was formed by use of a template as shown in the photograph of Figure 5. The template was controlled by guide strips with a slope along the channel of 0.00545 foot per foot. Four static disks connected to stilling wells, Figure 6, were installed on the center line of the channel at Stations 0+10, 0+30, 0+50, and 0+70 (Station 0+00 was near the channel entrance).

Velocity readings were obtained with a Pitot tube and cylinder bank, Figures 7 and 8a. The Pitot banks were designed to allow their location to be readily changed. A photograph of the Pitot banks mounted on the channel is shown in Figure 8b. The Pitot banks were connected by means of rubber or plastic tubing to a manometer board which was adjustable for various slopes, Figure 8c, and on the top Pitot tube were located taps for measuring static pressure for checking the static disk readings.

A standard mixture of aerosol and dye was used for bleeding the Pitot banks. Tube calibration was checked with the standard mixture

for the slope set on the manometer board, and Pitot tubes and cylinders were bled in a reverse direction to remove all air from the system.

A 12-inch laboratory pump was used to pump water from a laboratory sump through the model, and water discharge was measured by Venturi meters to check the discharge determined from the velocity readings.

OPERATION OF THE MODEL

The general procedure used in conducting a test was as follows:

1. The model was slowly backfilled.
2. The desired discharge was slowly set.
3. While the discharge was being set, a near constant water surface elevation was maintained at Station 0+66.
4. The model was operated continuously for an approximate 24-hour period.
5. While the model was being operated, point velocities were determined by means of the Pitot banks. Velocities were taken throughout a vertical half section of the channel at Station 0+66, and as near the boundary as possible. Velocity profiles were taken at 4-inch intervals across the right side of the channel (looking downstream) and the tubes and cylinders were frequently interchanged to check results.
6. At frequent intervals, the hook gage elevations in the wells connected to the static disks were obtained and the discharge was checked.

7. After 24 hours, the model was turned off and slowly drained.
8. After draining, the material which had deposited in the tail box was collected and weighed. It was then mixed and a sample was taken for analysis.
9. Cross sections were obtained at Stations 0+10, 0+30, 0+50, and 0+70.
10. Point samples of the sand-gravel mixture around the perimeter and on the channel center line were taken and analyzed.
11. Observations were made during and after each run and photographs were obtained.
12. Samples were replaced for the next test.

A discharge of 3.70 cubic feet per second was set for the first test. The discharge was gradually increased for each additional test. Eight tests were conducted, and the final discharge was 8.25 cubic feet per second.

DATA OBTAINED

Average discharges are shown in Table 1, and relative water surface elevations, obtained from hook gage readings, are shown in Table 2. Figure 9 shows channel cross sections, which gradually developed throughout the tests, and pertinent test data are listed in Table 3.

Point velocities obtained from Pitot readings may be obtained from reference (5), and a typical series of velocity profiles are shown plotted in Figure 10.

ANALYSIS OF DATA

Average Tractive Force

Before and after each test, cross sections were obtained at Stations 0+10, 0+30, 0+50, and 0+70, and during tests a number of water surface elevations were obtained at each of these stations. Following tests, average channel cross sections were plotted and the area of flowing water (A), wetted perimeter (P), hydraulic radius (R), average velocity at the station (V_a), and the velocity head (h_v) were determined.

Writing Manning's equation in the form

$$S_e = \left[\frac{V_a^2}{1.49^2 R^{4/3}} \right] n^2$$

the slope of the energy gradient, S_e , is indicated as a function of the roughness, n . As V_a and R were known, a value of n was assumed and S_e calculated at each station. Using the average of the S_e values at any two stations for the average energy slope occurring between these stations, a water surface profile was calculated (by starting at any given point) and compared with the measured water surface. Using the n value which resulted in a calculated water surface which most closely fitted the measured water surface, the S_e values at Stations 0+10, 0+30, 0+50, and 0+70 were determined. Average tractive forces, τ_e , were then calculated from the formula:

$$\tau_e = \gamma R S_e$$

Curves were drawn through the points, resulting in the graph, Figure 11, of the average tractive force acting along the channel.

Velocity Profiles from Point Velocities

During each test, velocities were obtained by the Pitot tube and cylinder banks, Figure 7. When obtaining velocities, the banks were set in the desired location and allowed approximately 5 minutes to stabilize. Approximately four manometer readings were obtained at each position at 5-minute intervals. If manometer readings indicated a continued change during this time, additional readings were obtained until stability occurred. Numerous velocity readings were obtained in the lower portion of the flow near the boundary (below 0.4 depth), and several readings to help establish the velocity curve were obtained above 0.4 depth.

Depths for plotting velocities were determined from the position of the boundary at the time velocity readings were started at a given vertical, and velocities near the boundary were determined first. On side slopes, the velocity distribution normal to the boundary was plotted.

For all tests, the manometer board was sloped to increase the displacement created by the velocity head by a factor of 20, or:

$$d = 20 h_v = 20 \frac{V_p^2}{2g}$$
$$V_p = 1.794 \sqrt{d}$$

where:

d = displacement on sloping manometer board

h_v = velocity head

V_p = average velocity at the point

g = acceleration of gravity (assumed to be 32.2 feet
per second per second)

Velocity plots for all tests were made in the form of y/d versus the velocity, Figure 10, on semilog graph paper. Straight lines were found to generally fit the velocity points.

Tractive Forces Determined from Point Velocities

The equation

$$\tau_o = C [u_{y_2} - u_{y_1}]^2$$

where:

$$C = \frac{\rho}{\left[5.75 \log \frac{y_2}{y_1}\right]^2}$$

was used to determine the boundary shear from the point velocities.

To determine the boundary shear at a point where a vertical velocity distribution had been determined, points from the velocity curves were read so that

$$\frac{\frac{y_2}{d}}{\frac{y_1}{d}} = 1.746$$

Using the square of the difference of the two velocities, the shear acting at the boundary was determined.

Average tractive force distributions are shown plotted in relation to the channel boundary in Figures 12 and 13, and plotted in a dimensionless form for comparison in Figure 14.

For the points shown on Figure 14, a quadratic equation of best fit was determined to be

$$\mathcal{T}_r = 1.27 + 1.05 D_r - 2.31 D_r^2$$

where:

\mathcal{T}_r = ratio of tractive force acting at a boundary point
divided by the average tractive force.

D_r = distance of the boundary point from the channel
center line divided by total distance from
center line to water surface edge.

As shown by Figure 14, the distribution was erratic for each test, but did show a general trend. Because of the general trend, a quadratic equation was fitted to the data by the least squares method.

Inspection of Figure 14 shows a maximum condition in the best fit curve occurring to the right of the center line. This may have been due to secondary currents. Its position may readily be determined from the derivative, as $D_r = 0.227$, at which point $\mathcal{T}_r = 1.38$. This would indicate that a tractive force 1.38 above the average generally occurred in the channel.

The standard deviation for the data plotted was determined to be 0.28, indicating that in the channel tested tractive forces, as determined by this method from the velocity distributions, usually fell in the range

$$\tau_r = 1.27 + 1.05 D_r - 2.31 D_r^2 \dots \pm 0.28$$

where units are as previously defined.

Data indicate that, generally, the average maximum tractive force occurring on the channel bottom as determined by this method in this channel was approximately 38 percent greater than τ_{RS_e} , and as the side slope started at approximately half the distance to the water surface edge, that average values approximately 22 percent greater than τ_{RS_e} occurred on the side slope. These forces are larger than those usually thought of as maximum tractive forces occurring on the boundary.

Comparison of Average Tractive Force Determined by $\tau_a = \tau_{RS_e}$ and Average Tractive Force Determined from Velocity Distribution

Assuming a linear distribution of tractive forces between points at which the boundary shear was determined, an average tractive force from point velocity data were determined from

$$\tau_e = \frac{\sum_{i=1}^n \tau_i \Delta L_i}{L}$$

where:

τ_i = the average tractive force occurring over interval ΔL_i

L = total length of wetted perimeter over which velocities were measured

n = number of intervals

The average tractive force obtained by this method is given in Table 1, as is the average tractive force obtained from $\mathcal{T}_a = \mathcal{I} R S_e$. Figure 15a shows a plot of the two average tractive forces. In general, there appears to be no consistent trend for tractive forces obtained from point velocities to be either higher or lower than those obtained by the conventional formula. The tractive forces obtained from the point velocities are more erratic than those obtained from the conventional formula. This is understandable because of the sensitivity of the tractive force to the velocity gradient. In general, a slight change in the velocity gradient will result in a considerable change in the magnitude of the tractive force. If insufficient velocity points are determined, the tractive force obtained from this method would be of questionable value.

Change in Roughness of Channel

As the tests progressed, the roughness of the channel increased. The increase in roughness was probably due in part to the finer material being transported from the surface and into the tail box, while larger material stayed in place. Figure 15b shows the roughness increase plotted in terms of Manning's n value. As may be noticed, the value increased from 0.0144 to 0.0180.

DISCUSSION

Plots of point velocity data indicated the vertical velocity distribution closely followed a logarithmic form. Secondary currents

were neglected in the study, and it is assumed they had little effect on the results.

A large source of error in determining the tractive force distributions from point velocities can come from establishing the slope of the velocity gradient, as a slight error in slope will result in a considerable difference in the computed tractive force. For example, when the velocity gradient is near 70° from the horizontal, a 4 percent error in setting the slope would result in approximately 30 percent error when calculating the tractive force. Care should be taken in selecting a line through the velocity points, and numerous and accurate velocity points should be obtained when the velocity gradient is to be found by this method. Care must also be taken in establishing the point and the boundary, as for a given point near the boundary a small error in establishing the location of the boundary or point will result in a large error in the y/d value. For this reason, when operating with a movable bed, it is not always best to use the lowest points in establishing the velocity gradient. Points below 0.4 of the depths should be used, but if the curve has considerable deviation near the bottom-most points, the magnitude of the possible error should be checked.

Many attempts have been made to determine the distribution of tractive forces in an open channel. Lane (6) found the maximum

tractive force on the side slope to be equal to approximately $0.78 \tau dS_e$, and that on the bottom to approach τdS_e . Other investigators have determined the distribution of tractive forces varies with the side slope of the channel, but is unaffected by the size of the section.

CONCLUSIONS

On the basis of these tests and the analysis used in this report, it is concluded:

1. The velocity distribution in the open channel tested followed a logarithmic equation over the entire cross section.
2. Secondary currents of the magnitude encountered in the study did not appreciably affect the logarithmic equation.
3. Boundary shears, determined from point velocities, approached maximum values near the center of the channel, and were approximately 40 percent greater than the average tractive force as obtained from the formula, $\tau_a = \tau R S_e$.
4. Boundary shears, determined from point velocities, became less on the side slope, but near the toe of the slope still had average values greater than those obtained from $\tau_a = \tau R S_e$.
5. Boundary shears, determined from point velocities approached small values near the water surface edge.
6. Boundary shears distributed around the perimeter of the channel tested fluctuated considerably, with a standard deviation of approximately 28 percent from the average point value.

7. Distribution of average boundary shear across the channel cross section (determined from fitting a quadratic equation to the scatter diagram by the least squares method) followed the formula

$$\mathcal{T}r = 1.27 + 1.05 D_r - 2.31 D_r^2$$

where $\mathcal{T}r$ is a tractive force ratio and D_r is a distance ratio.

8. When computing boundary shears from point velocities, it is important to use numerous and accurate point velocities occurring below 0.4 depths. Location of the boundary and each velocity point should be accurately determined.

9. Average boundary shears computed from point velocities generally agreed with those computed from du Boys formula.

REFERENCES

1. Prandtl, F., "Über die ausgebildete Turbulenz," Proceedings of Second International Congress for Applied Mechanics, Zurich, 1926.
2. von Karman, Th., "Goettinger Nachrichten," Proceedings of Third International Congress for Applied Mechanics, Stockholm, 1930.
3. Keulegan, G. H., "Laws of Turbulent Flow in Open Channels," Journal of Research of the National Bureau of Standards, U. S. Department of Commerce, National Bureau of Standards, Research Paper RP1151, Volume 21, December 1938.
4. Einstein, H. A., "The Bed-Load Function for Sediment Transportation in Open Channel Flows," Technical Bulletin No. 1026, U. S. Department of Agriculture, September 1950.
5. Enger, P. "F.," "Tractive Force Distribution around the Perimeter of an Open Channel by Point Velocity Measurements," Master's Thesis, submitted to the University of Colorado, August 1960.
6. Lane, E. W., Progress Report on Results of Studies on Design of Stable Channels, Hydraulic Laboratory Report No. HYD-352, U. S. Department of the Interior, Bureau of Reclamation, June 1952.

TABLE I
DISCHARGES AND TRACTIVE FORCES COMPARED

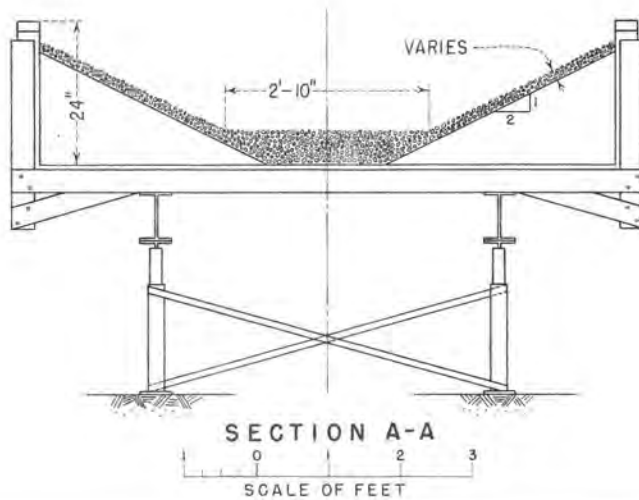
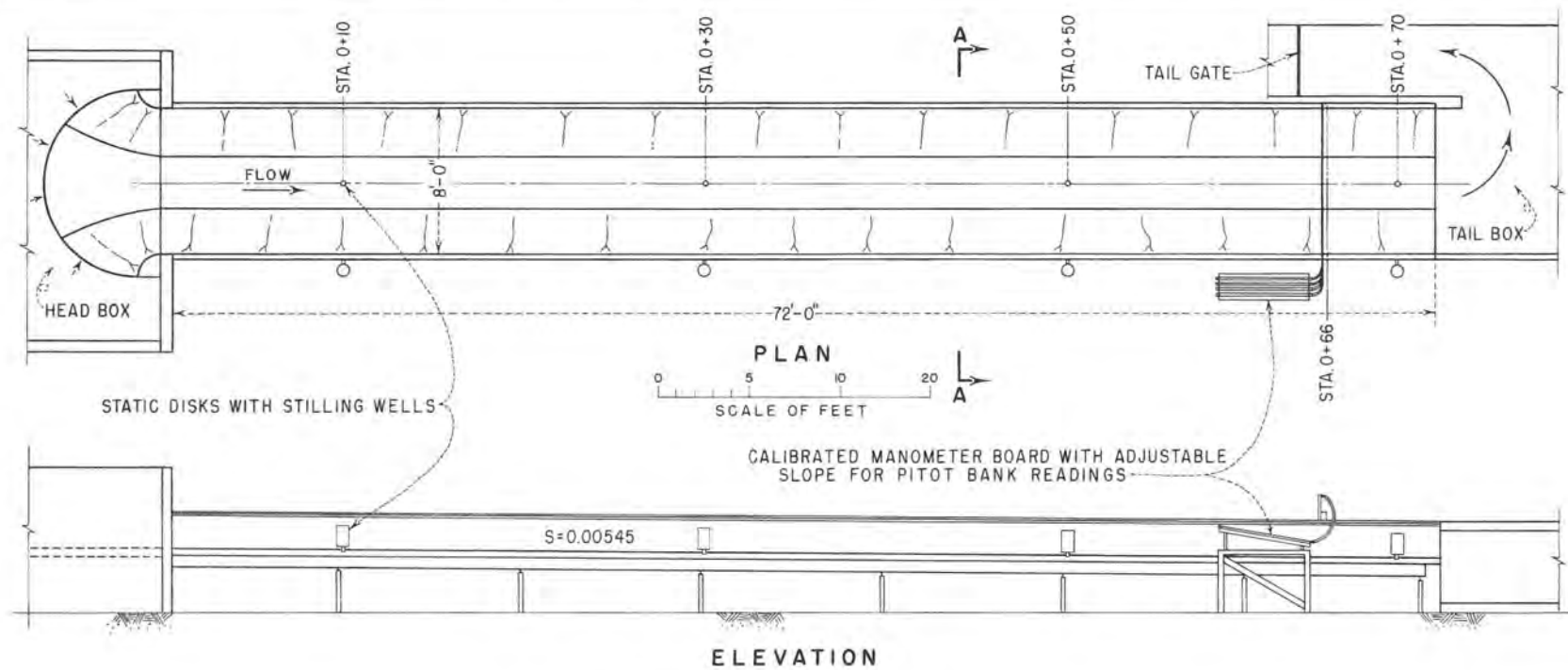
Test No.:	Discharge: : read on : Venturi : meter : cfs	Discharge: : calculated: : from : velocity : reading : cfs	Average : tractive : force : from : $T = \gamma R S_e$: at station: : 0+66 : 1b/ft ² : $\times 10^{-2}$	Average : tractive : force : from : $T = C(u_x - u_y)^2$: at station: : 0+66 : 1b/ft ² : $\times 10^{-2}$	Average : Manning's : "n" : value
1	: 3.70	: 3.64	: 0.65	: 0.84	: 0.0144
2	: 4.72	: 4.60	: 1.00	: 1.16	: 0.0144
3	: 5.51	: 5.60	: 1.33	: 1.22	: 0.0144
4	: 6.03	: 6.05	: 1.98	: 2.09	: 0.0150
5	: 6.62	: 6.77	: 2.55	: 3.12	: 0.0155
6	: 7.16	: 7.29	: 3.02	: 3.39	: 0.0155
7	: 7.70	: 7.66	: 4.33	: 4.03	: 0.0167
8	: 8.25	: 7.85	: 5.27	: 4.90	: 0.0180

TABLE 2
RELATIVE WATER SURFACE ELEVATIONS

Test No. :	Station :0+10.....	Station :0+30.....	Station :0+50.....	Station :0+72.....
1	5.8381	5.8373	5.8424	5.8415
2	5.7628	5.8515	5.8528	5.8574
3	5.8660	5.8534	5.8544	5.8570
4	5.8678	5.8438	5.8440	5.8387
5	5.8746	5.8508	5.8425	5.8367
6	5.9031	5.8770	5.8680	5.8572
7	5.8860	5.8498	5.8309	5.8118
8	5.9134	5.8840	5.8589	5.8338

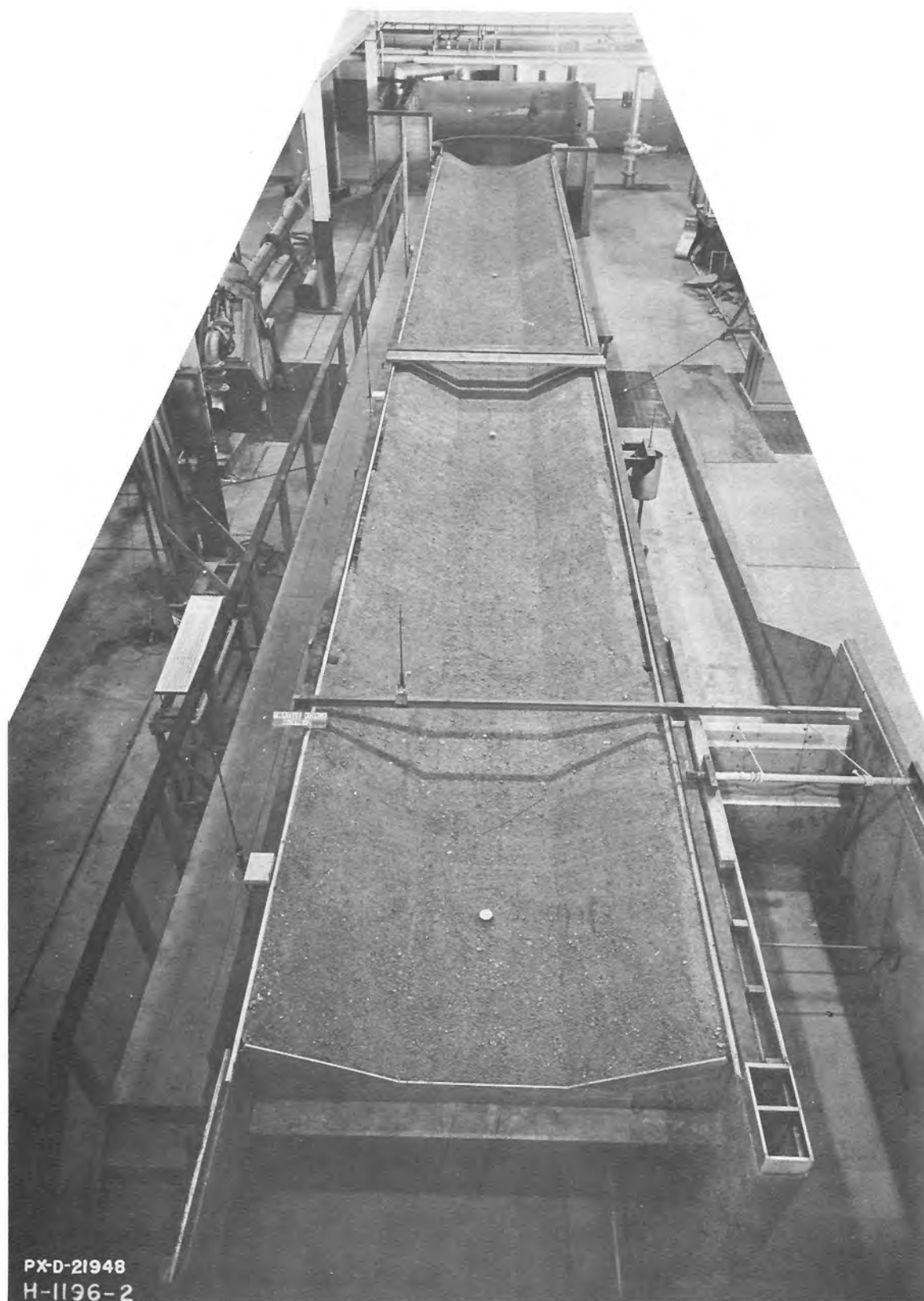
Table 3

		: Wetted		: Hydraulic	Average	
Test:	Station:	perimeter,	Area,	radius,	velocity,	$\frac{V^2}{2g}$
:	:	feet	ft ²	feet	ft/sec	x 10 ²
1	: 0+10	: 5.46	: 2.31	: 0.423	: 1.60	: 3.97
	: 0+30	: 5.73	: 2.79	: 0.487	: 1.33	: 2.74
	: 0+50	: 6.17	: 3.32	: 0.538	: 1.11	: 1.91
	: 0+72	: 6.73	: 4.06	: 0.603	: 0.911	: 1.29
2	: 0+10	: 5.40	: 2.16	: 0.400	: 2.19	: 7.24
	: 0+30	: 5.86	: 2.85	: 0.487	: 1.65	: 4.25
	: 0+50	: 6.21	: 3.41	: 0.549	: 1.38	: 2.97
	: 0+72	: 6.82	: 4.19	: 0.614	: 1.13	: 1.98
3	: 0+10	: 5.48	: 2.44	: 0.445	: 2.26	: 7.95
	: 0+30	: 5.98	: 3.02	: 0.505	: 1.82	: 5.17
	: 0+50	: 6.41	: 3.56	: 0.555	: 1.55	: 3.72
	: 0+72	: 6.88	: 4.20	: 0.610	: 1.31	: 2.68
4	: 0+10	: 5.92	: 2.58	: 0.436	: 2.33	: 8.46
	: 0+30	: 6.03	: 2.91	: 0.482	: 2.07	: 6.67
	: 0+50	: 6.47	: 3.39	: 0.524	: 1.78	: 4.92
	: 0+72	: 6.72	: 3.90	: 0.581	: 1.54	: 3.71
5	: 0+10	: 5.68	: 2.80	: 0.493	: 2.36	: 8.66
	: 0+30	: 6.06	: 3.20	: 0.528	: 2.07	: 6.63
	: 0+50	: 6.28	: 3.38	: 0.538	: 1.96	: 5.95
	: 0+72	: 6.98	: 3.94	: 0.564	: 1.68	: 4.52
6	: 0+10	: 5.75	: 2.73	: 0.475	: 2.62	: 10.7
	: 0+30	: 6.22	: 3.23	: 0.519	: 2.22	: 7.60
	: 0+50	: 6.46	: 3.49	: 0.540	: 2.05	: 6.60
	: 0+72	: 7.00	: 3.86	: 0.551	: 1.86	: 5.40
7	: 0+10	: 6.06	: 3.04	: 0.501	: 2.53	: 10.0
	: 0+30	: 6.17	: 3.21	: 0.520	: 2.40	: 8.90
	: 0+50	: 6.51	: 3.53	: 0.542	: 2.18	: 7.40
	: 0+72	: 6.76	: 3.66	: 0.542	: 2.10	: 6.80
8	: 0+10	: 6.22	: 3.05	: 0.490	: 2.70	: 11.3
	: 0+30	: 6.33	: 3.38	: 0.533	: 2.44	: 9.25
	: 0+50	: 6.62	: 3.67	: 0.555	: 2.25	: 7.83
	: 0+72	: 6.96	: 3.83	: 0.550	: 2.15	: 7.19



GENERAL PLAN OF FLUME USED
FOR TRACTIVE FORCE STUDY

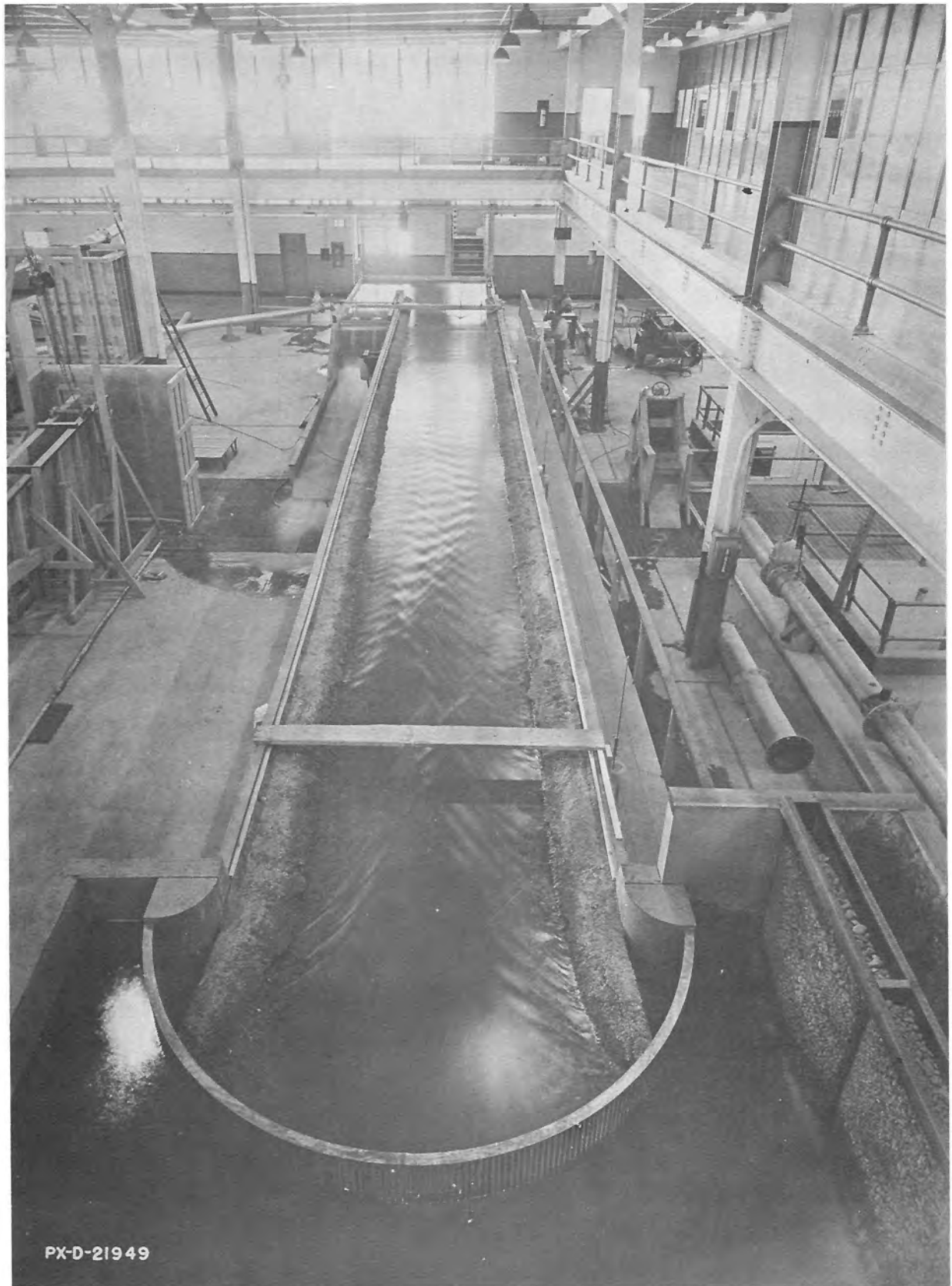
Figure 2



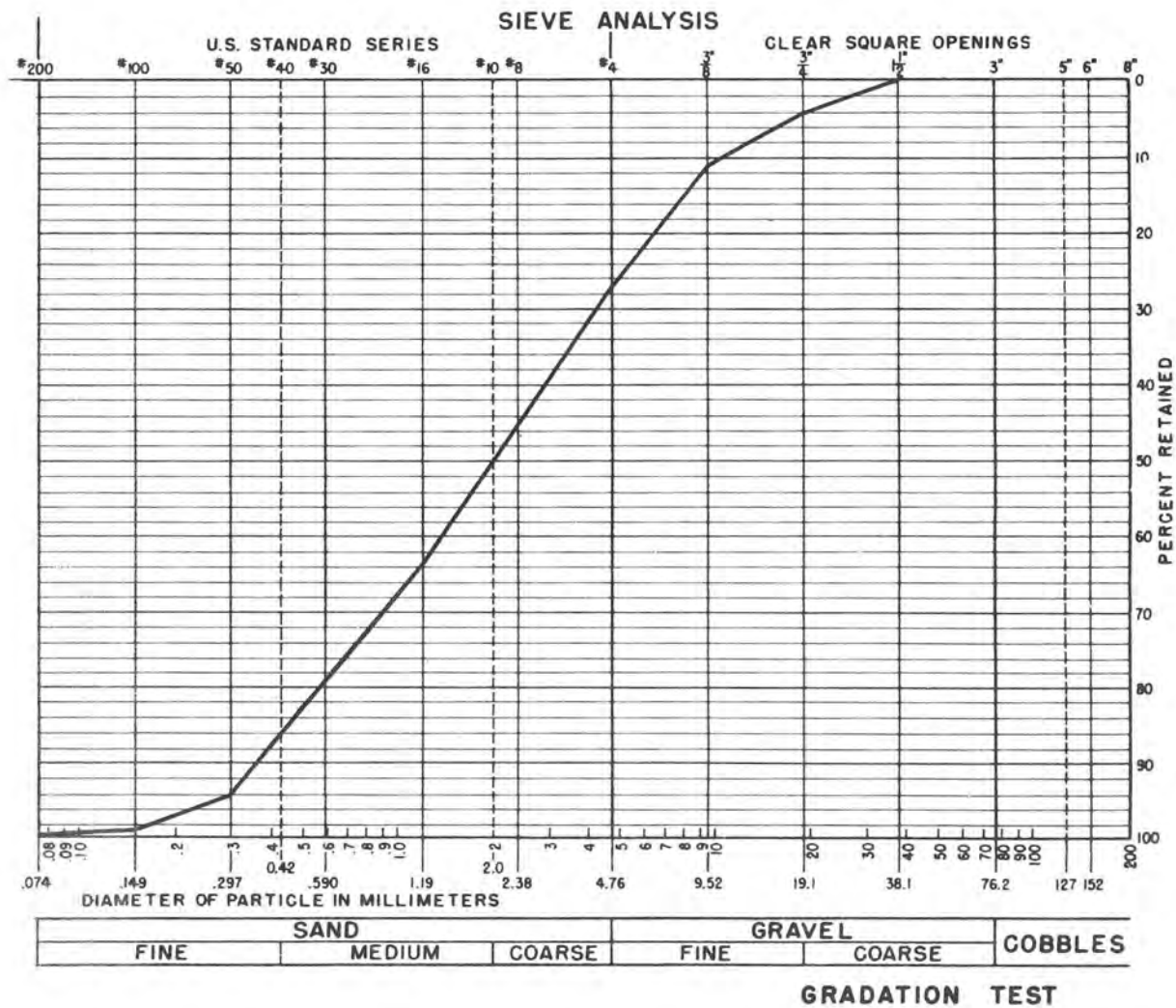
PX-D-21948
H-1196-2

FLUME PREPARED FOR TEST 1

Figure 3



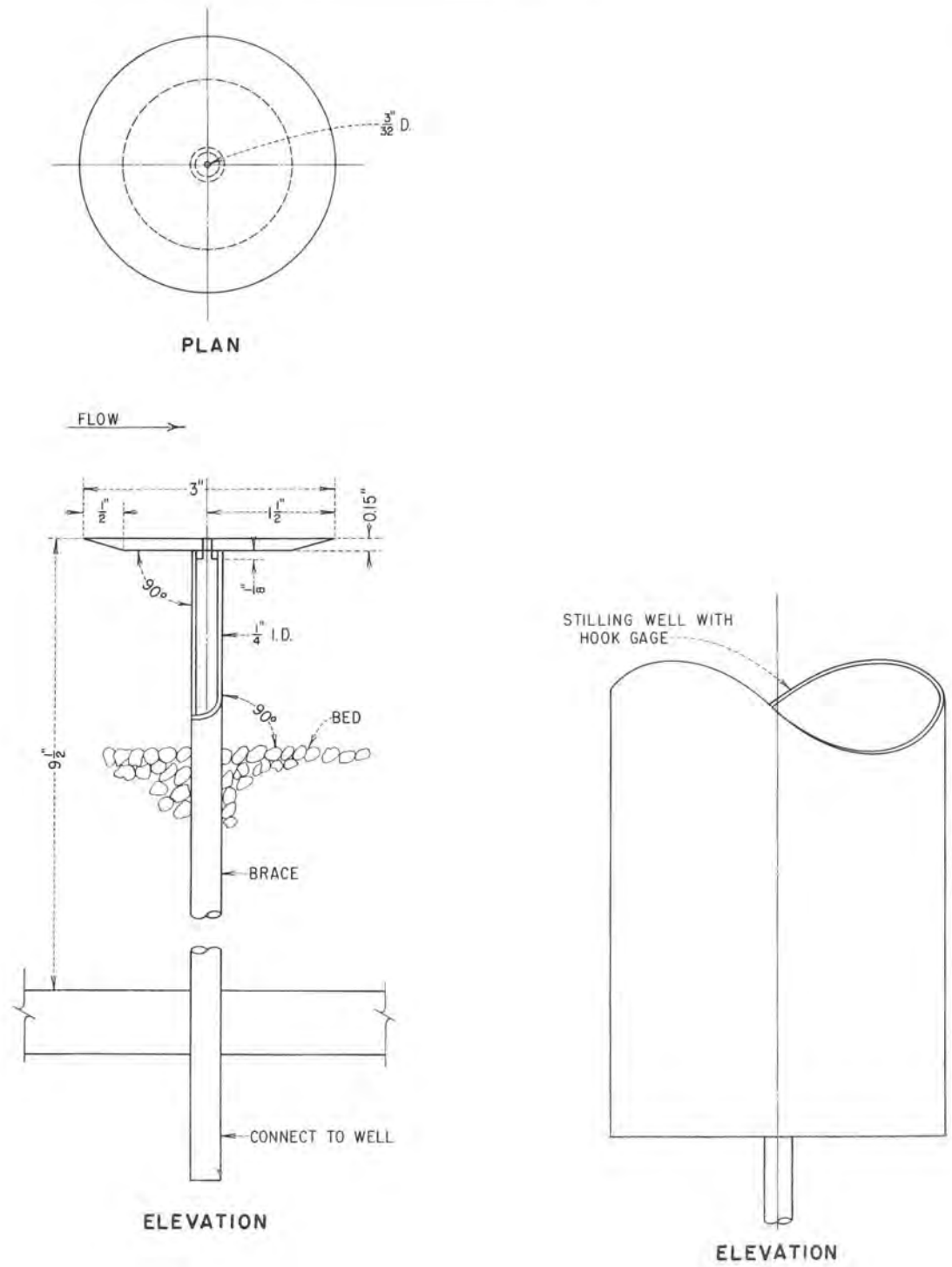
MODEL IN OPERATION DURING TEST 5



ANALYSIS CURVE OF MATERIAL USED FOR STUDY

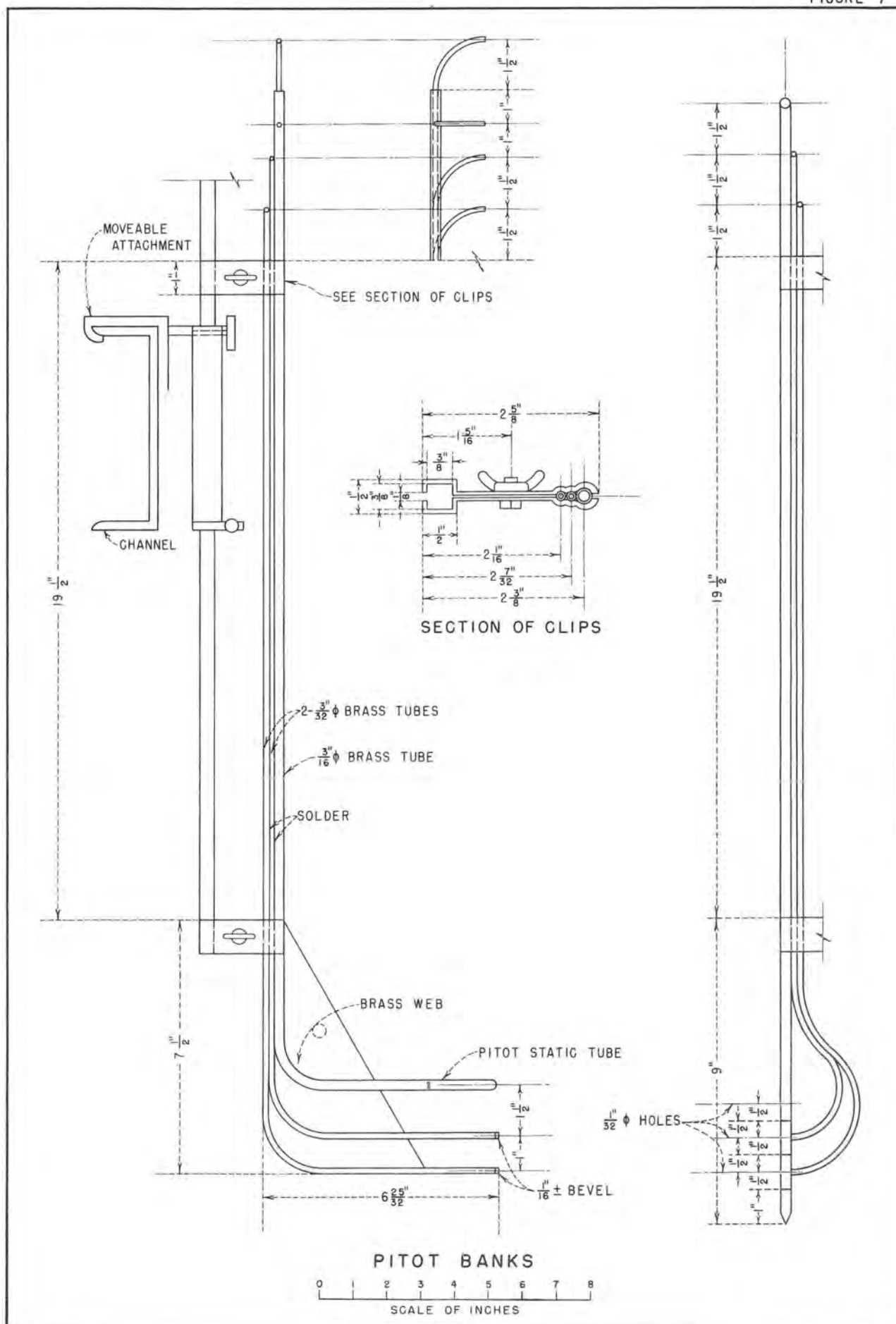


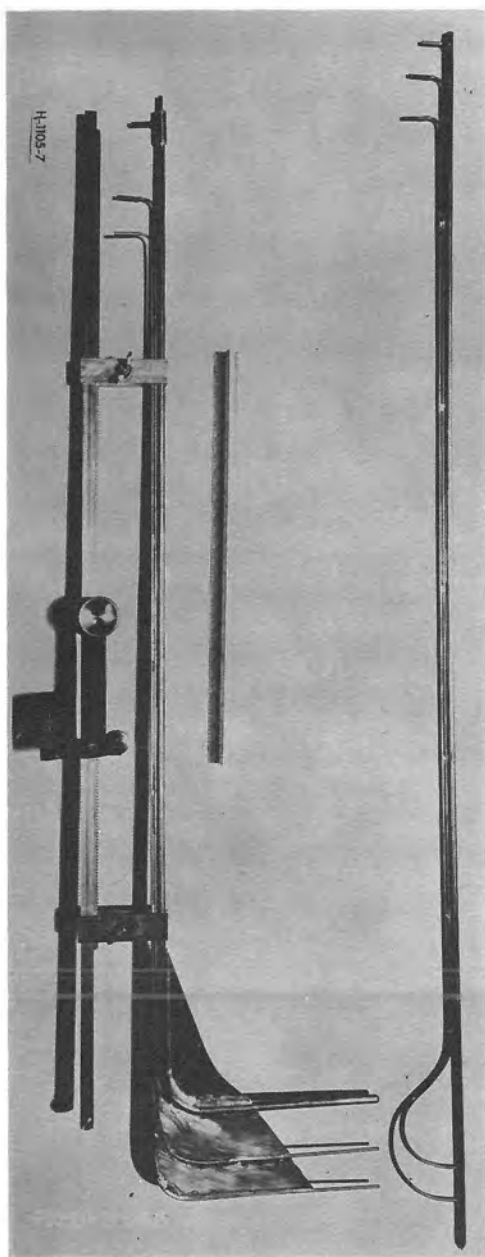
TEMPLATE USED FOR SHAPING CHANNEL



STATIC DISK

FIGURE 7





(a)
Pitot Tube and
Cylinder Bank

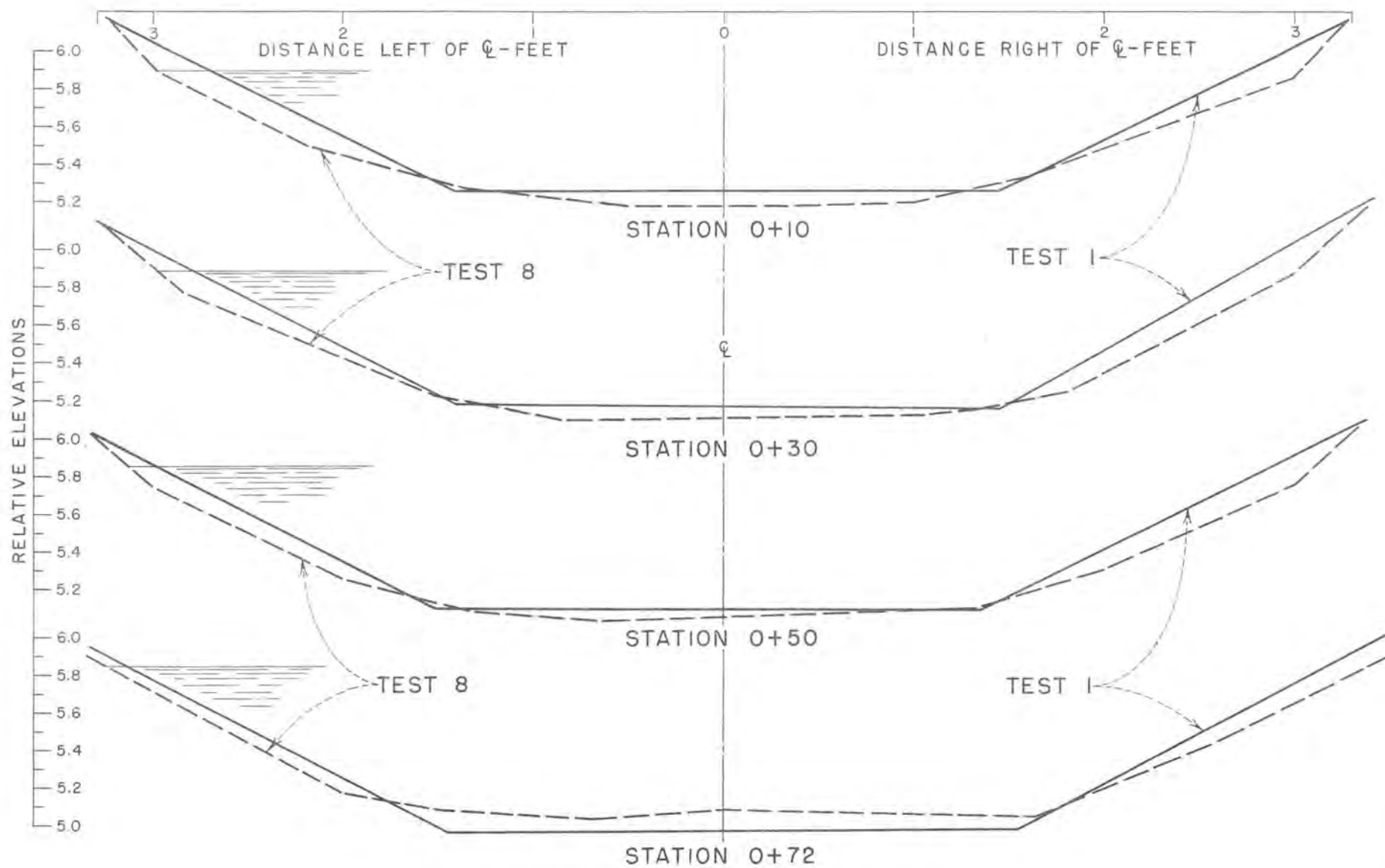


(b)
Mounted Pitot Banks



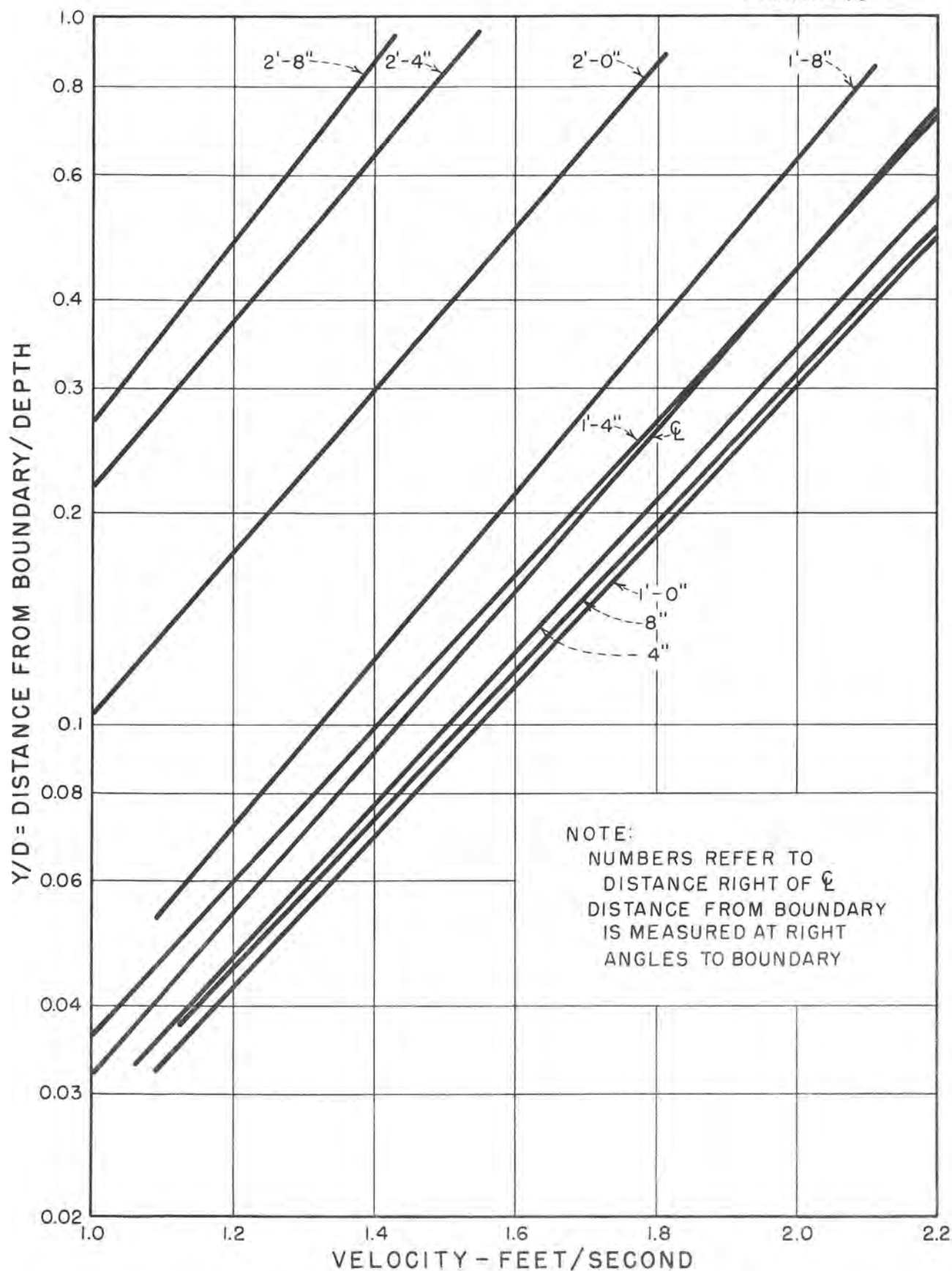
(c)
Sloping Manometer Board

PITOT TUBES AS OPERATED

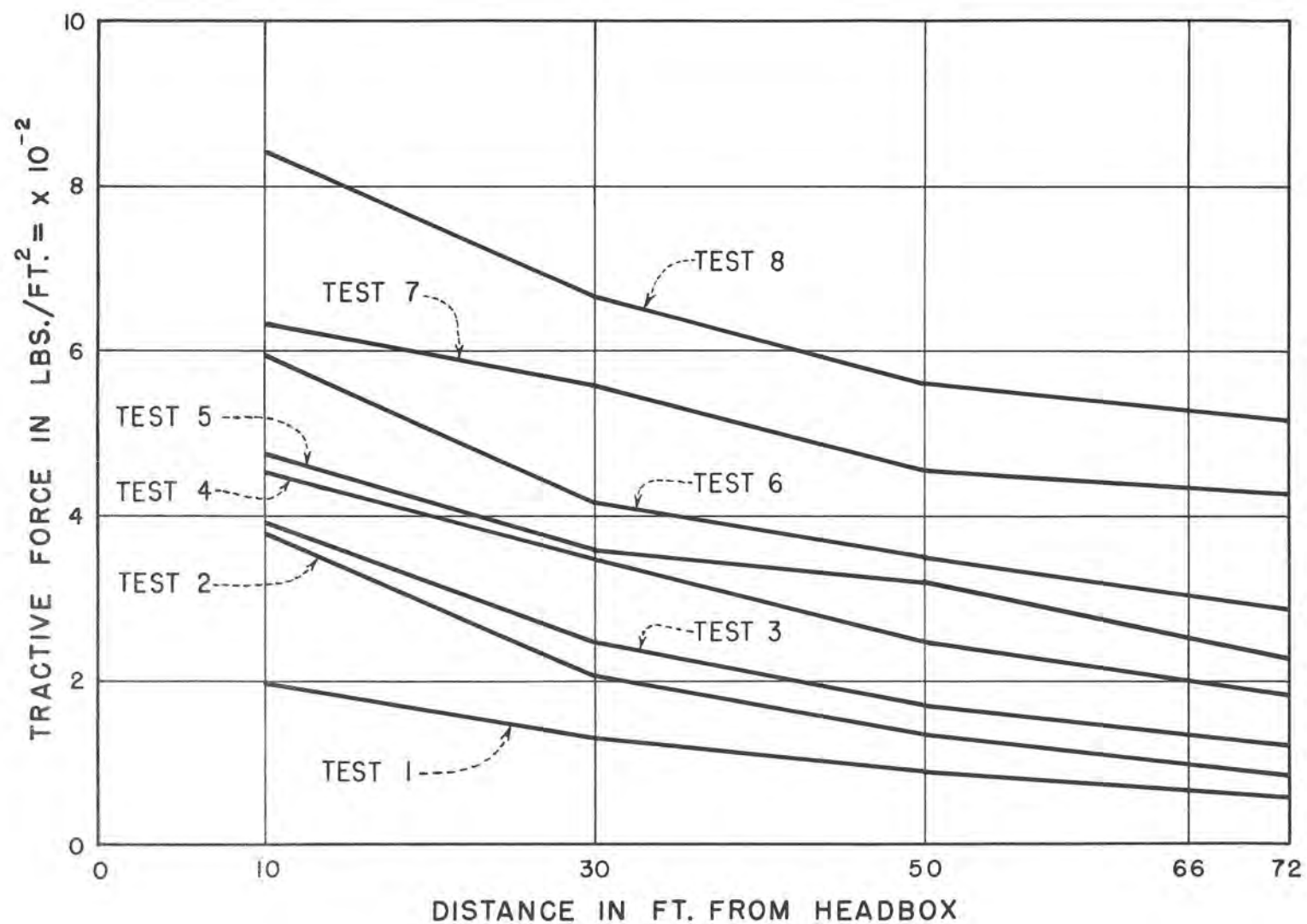


CROSS SECTION CHANGES DURING TESTS

FIGURE 10

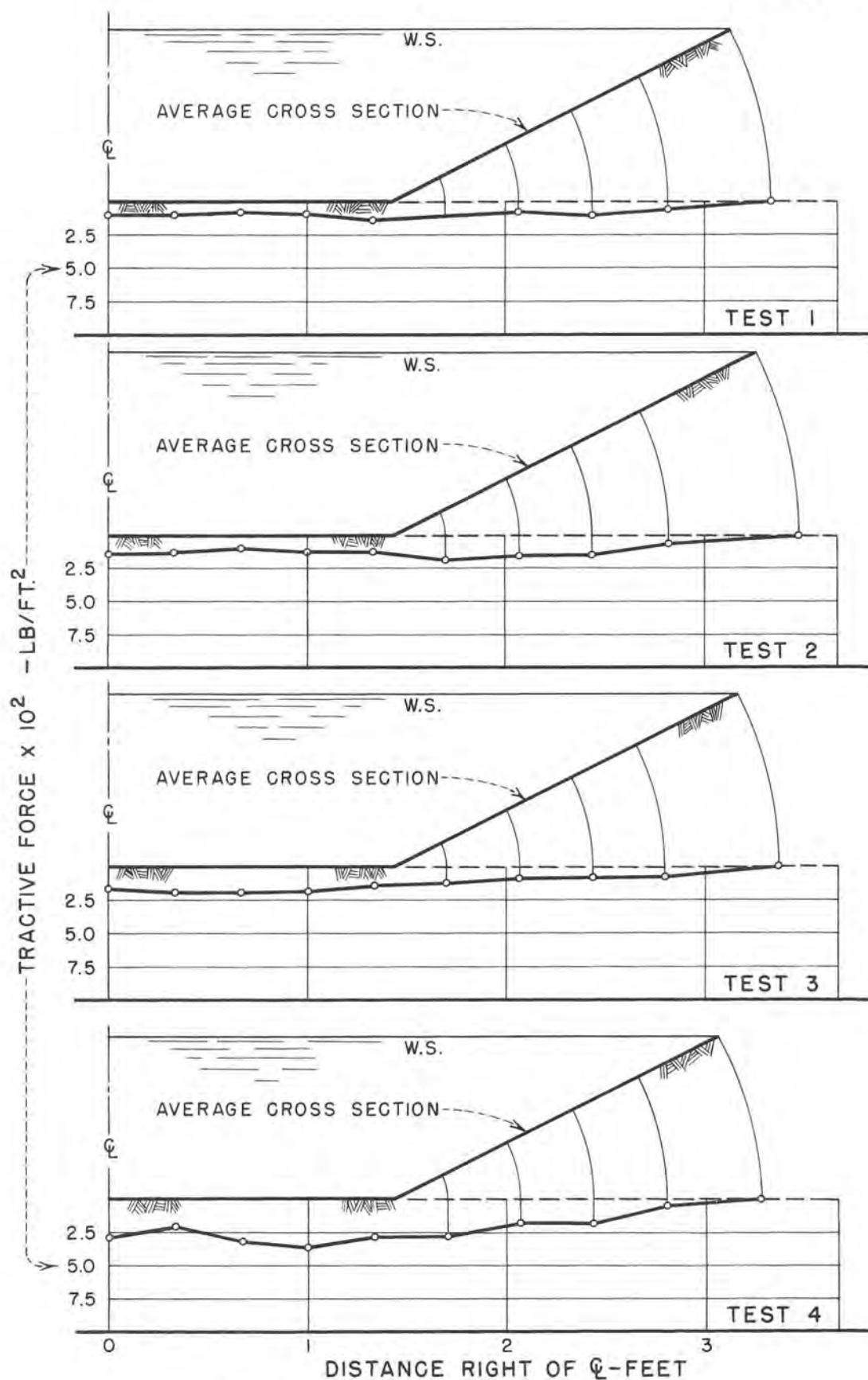


VELOCITY PROFILES FOR TEST 5



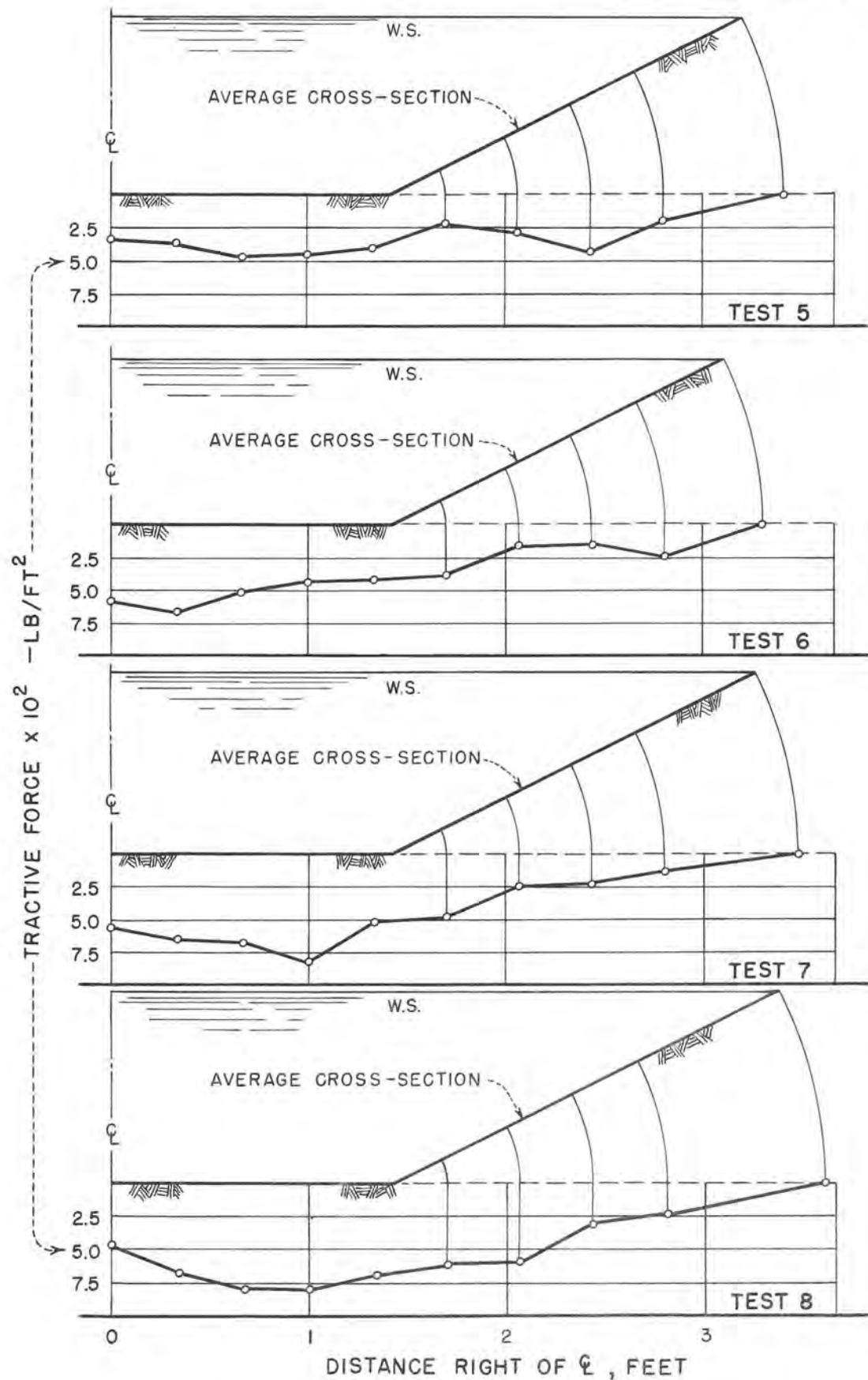
TRACTIVE FORCE VARIATION ALONG CHANNEL

FIGURE 12

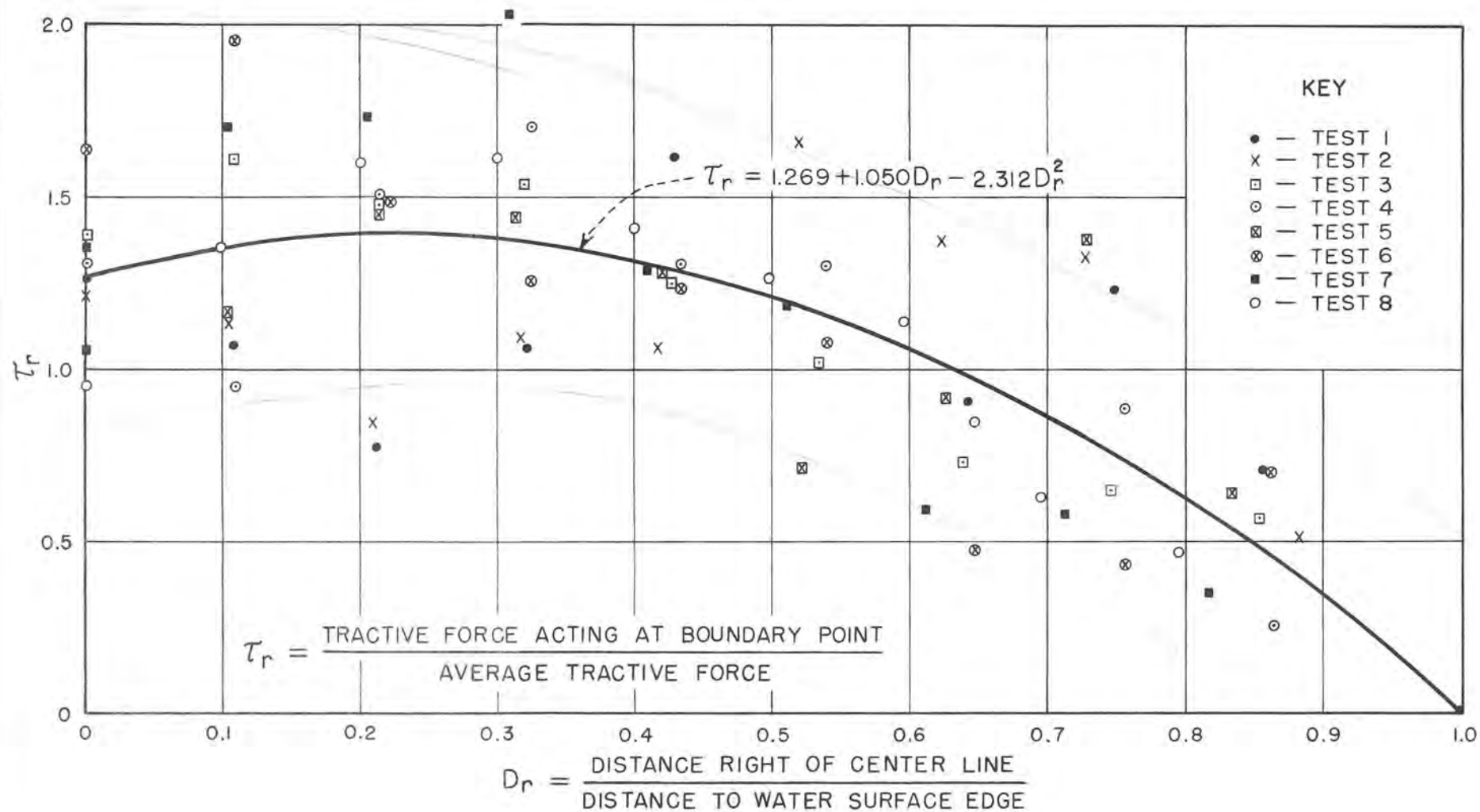


TRACTIVE FORCE DISTRIBUTIONS
TESTS 1 THROUGH 4

FIGURE 13

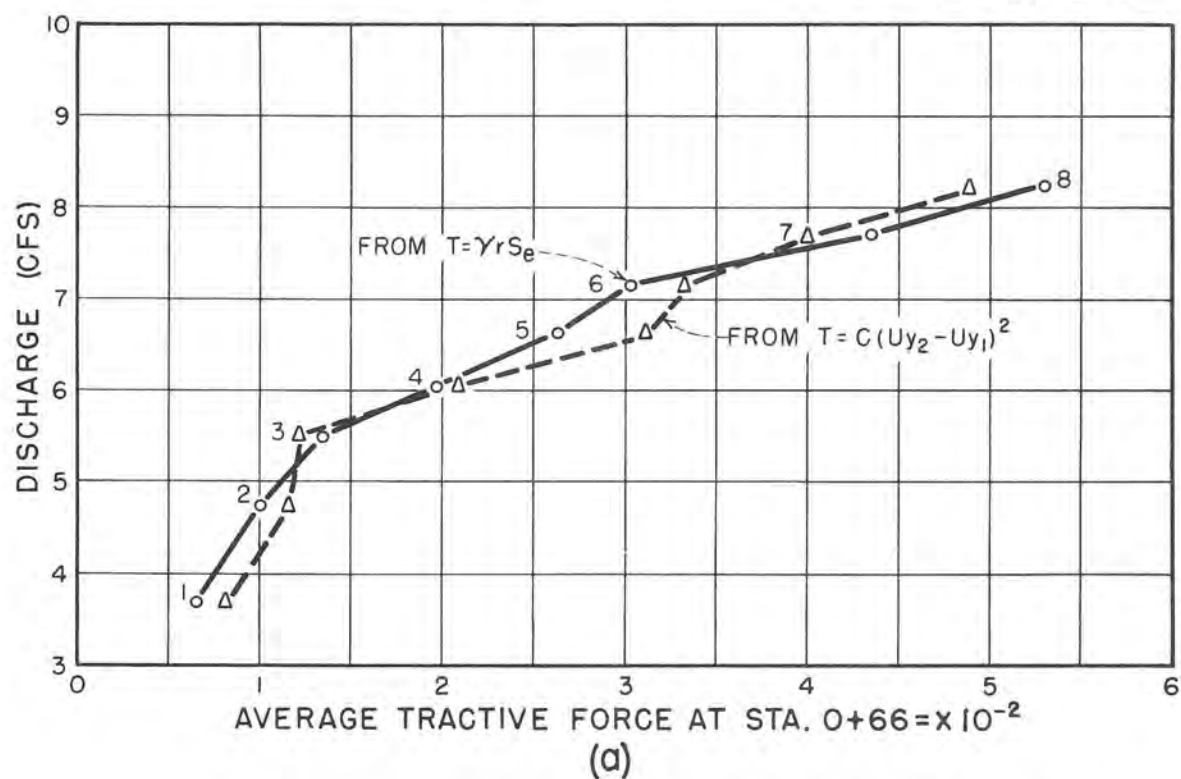


TRACTION FORCE DISTRIBUTIONS
TESTS 5 THROUGH 8

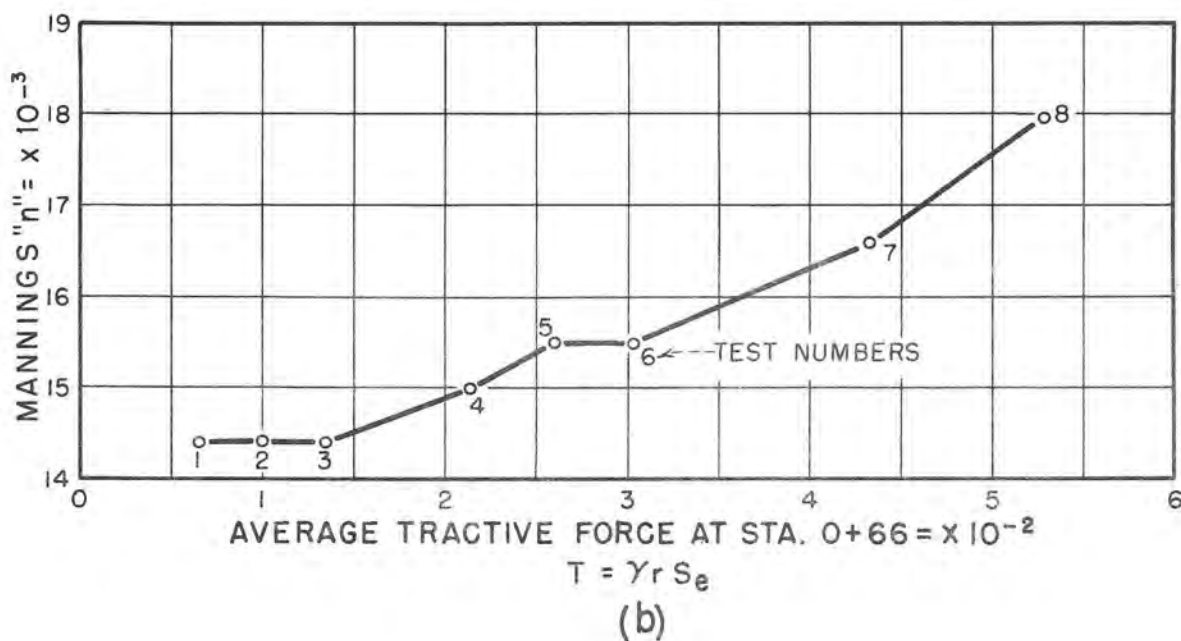


TRACTIVE FORCE DISTRIBUTION

FIGURE 15



TEST	1	2	3	4	5	6	7	8
MANNING'S "n" VALUE	0.0144	0.0144	0.0145	0.0150	0.0153	0.0156	0.0167	0.0180



COMPARISON OF THE AVERAGE TRACTIVE FORCE
FROM THE TWO METHODS
AND INCREASE IN MANNING'S "n" VALUE

